Power Electronic Systems
Laboratory

Proceedings of the 15th European Conference on Power Electronics and Applications and Exhibition (EPE'13-ECCE Europe), Lille, France, September 3-5, 2013

Acoustic Noise in Inductive Power Components

J. Mühlethaler,
M. Schubiger,
U. Badstübner,
J. W. Kolar

ETH
Eidgenössische Technische Hochschule Zürich
Swiss Federal Institute of Technology Zurich

Acoustic Noise in Inductive Power Components

Jonas Mühlethaler*, Manuel Schubiger†, Uwe Badstübner‡, and Johann W. Kolar§
*Gecko-Simulations AG, Zurich, Switzerland, Email: jonas.muehlethaler@gecko-simulations.com
†ABB Switzerland Ltd., Power Electronics, Turgi, Switzerland
‡ABB Switzerland Ltd., Corporate Research, Baden-Dättwil, Switzerland
§Power Electronic Systems Laboratory, ETH Zurich, Switzerland

***Abstract*—This paper deals with the acoustic emissions of PWM-operated inductive components in the medium frequency range. It is shown with measurements that the noise emissions are primarily caused by magnetostriction, an induction-dependent dimensional change of the magnetic core. The influences of various modulation parameters on the sound pressure level spectra of two prototypes are measured and analyzed. It is confirmed that the emitted sound is proportional to the square of the magnetic flux density.**

I. Introduction

In case magnetic components in power electronic systems are operated at switching frequencies in the audible range, a disturbing operating noise is perceived. The easiest measure to avoid this noise is to select a switching frequency above the audible range. However, since the losses in power electronic systems generally increase with an increase of the switching frequency, this is not always possible. Thus, for many applications, the emitted noise spectrum is within the audible range.

In literature, this well-known phenomenon is mainly discussed in connection with grid-transformers operated at $50/60\,\mathrm{Hz}$ [1]–[4], and only few publications discussing higher frequency ranges have been found [5]–[7]. In [5] and [6] Sound Pressure Level (SPL) measurements are presented and guidelines, how to design low-noise inductive power components, are given. In [7], resonance effects in laminated cores of grain-oriented electrical steel are discussed. More information about acoustic noise emission can be found in publications about electrical machines, e.g. [8]–[10]. However, to the author's knowledge, a general model that allows the prediction of acoustic noise in inductive components hasn't been established yet. Therefore, a research project has been initiated with the goal to enable acoustic measurements and, thus, to gain understanding about acoustic noise in magnetic components employed in the mentioned frequency range. In this paper, firstly, measurement results are presented that allow to determine the acoustic noise source, i.e. magnetic forces on windings, magnetic forces between core laminations, or magnetostriction. Secondly, the influence of various parameters, such as the peak-to-peak flux density B_{pp}, the frequency f_{s}, a DC premagnetization B_{DC}, and the duty cycle D, is analyzed. In order to determine the parameter dependency, the sound pressure level spectra of two prototypes have been measured in the medium frequency range ($\approx 1 \ldots 20\,\mathrm{kHz}$).

The structure of the paper is as follows: a brief theoretical summary about different noise sources is given in Section II. The acoustic measurement system is discussed in Section III, in Section IV and Section V the influence of the flux profile on the acoustic noise emissions is analyzed, and in Section VI the results are discussed and the paper is concluded.

II. Theory

Acoustic noise origins in mechanical vibrations of inductive components. If the mechanical parts oscillate at a frequency in the audible range (between 20 Hz and 20 kHz), a disturbing tone is emitted. The three main noise sources are the vibrations of windings due to magnetic forces acting on the winding (cf. Section II-C), vibrations of core due to magnetic forces between laminations (cf. Section II-B), and the change of the core dimensions, i.e. magnetostriction (cf. Section II-A).

A. Magnetostriction

The phenomenon of a change of the core dimensions due to an applied magnetic field is called magnetostriction. Normally, the core changes its length in the direction of the applied field, whereas the volume stays approximately constant. This relative change in length is described as

$$\lambda = \frac{\Delta l}{l} \frac{\mu m}{m}, \tag{1}$$

where Δl is the change of the length l. A measure of the magnetostriction is the so-called saturation-magnetostriction λ_{s}. λ_{s} describes the relative longitudinal change in length of a magnetically saturated material. The saturation-magnetostriction differs for different materials and is in the range of few $\mu\mathrm{m}/\mathrm{m}$. If the saturation-magnetostriction is reached, an increase of the applied magnetic field leads to a volume-magnetostriction. However, this effect is negligible [11, p. 241 ff.]. Accordingly, in order to minimize the acoustic noise, a core material with a low saturation-magnetostriction λ_{s} is preferable.

An applied ac magnetic field leads to a periodic deformation of the core with twice the magnetic field frequency. The reason for doubling the frequency is that the change in length of the core is the same for both magnetization half waves (i.e. magnetization directions). The magnetostriction follows a nonlinear, material-specific function of the magnetic flux density. However, below the magnetic saturation the magnetostriction can be simplified as a square function of the magnetic flux density [1], [5].

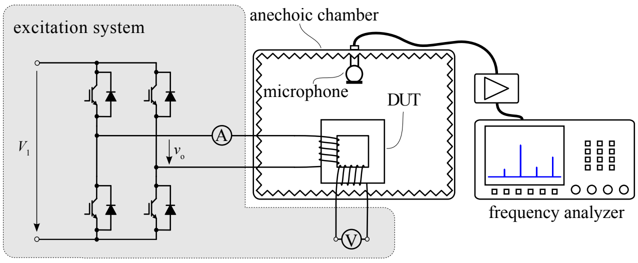

Fig. 1. Test setup to measure the Sound Pressure Level (SPL).

B. Magnetic Forces Acting on Core

An additional source of acoustic noise are vibrations due to magnetic forces acting on the core. If the boundary surfaces between two core parts are parallel to the magnetic flux density, the resulting magnetic forces are negligible. But, if the magnetic flux density has a component orthogonal to the boundary surfaces, e.g. near an air gap, the magnetic forces are much bigger. The resulting force between two core parts is proportional to the square of the magnetic flux density. In case of insufficient mechanical fixation of the core parts, the acting forces lead to a sound emission [1].

C. Magnetic Forces Acting on Windings

A current leads to a magnetic field and, accordingly, magnetic forces are occurring between the turns of a winding. These forces may lead to vibrating and sound emitting windings. However, according to [2], [5], with common current densities the vibration can be prevented with an adequate fixation of the windings.

D. Relevance of the Acoustic Noise Sources

The main magnetic noise sources are the vibrating cores, whereas the forces that act on magnetic windings are presumably less pronounced. These core vibrations are due to magnetic forces between laminations and magnetostriction, whereas it is expected that the magnetostriction is the dominating phenomenon. Another relevant finding for the analysis of acoustic noise presented in the literature is that the emitted sound is proportional to the square of the magnetic flux density [6].

III. Test Setup

An acoustic measurement system has been built in order to measure the Sound Pressure Level (SPL) and its frequency spectrum. This acoustic measurement system is an extension to an existing system that has been used for the measurement of core losses in inductive components [12]. The acoustic measurement system is illustrated in Fig. 1. The Device Under Test (DUT) is placed in an anechoic chamber and is driven by an H-bridge that is applying a rectangular voltage to the DUT. This excitation leads to a sound emission. At a distance of 25 cm to the DUT, a measurement condenser microphone converts the SPL into an electric signal. This signal is then, via a microphone amplifier, transferred to a frequency analyzer in order to determine its frequency spectrum. In the following paragraphs, first, the quantity to be measured and, below, the components of the test system are introduced in detail.

A. Measured Variable

The vibration of the inductive components leads to a sound emission. Sound is a small change in air-pressure that is superimposed to the atmospheric air-pressure. The human ear is capable of hearing frequencies between approximately 20 Hz and 20 kHz.

The physical quantity to be measured is the sound pressure level (SPL) [13, p. 47 ff.]. The SPL S_p in dB is calculated as

$$S_\mathrm{p} = 20\log\left(\frac{p_\mathrm{eff}}{p_0}\right), \tag{2}$$

where p_eff is the rms value of the actual sound pressure and $p_0 = 2\times10^{-5}\,\mathrm{Pa}$ is the reference sound pressure. The reference sound pressure p_0 corresponds approximately to the human hearing threshold level at 1 kHz.

The SPL is easy measurable with microphones. However, if the measured SPL is used to quantify acoustic noise, a clearly defined measurement setup is needed. For instance, in this work all acoustic measurements have been conducted at a test distance between DUT and microphone of 25 cm.

B. Excitation of Device Under Test

In power electronics systems, often rectangular voltages are applied across inductive components. This leads to a triangular shaped (or piecewise-linear) current and, accordingly, to a triangular flux density time behavior inside the inductive component. The H-bridge of the test system described above is capable of a maximum input voltage of $450\,\mathrm{V}$, maximum output current of $25\,\mathrm{A}$ and a switching frequency of up to $200\,\mathrm{kHz}$. The duty cycle and the dc current (i.e. a dc premagnetization B_DC) can be changed.

The magnetic flux density $B(t)$ is a characteristic value for the acoustic noise emission. Therefore, a sense winding (secondary winding) is added to the core. The voltage across the sense winding is integrated to sense the core flux density B as

$$B(t) = \frac{1}{N_\mathrm{s}\cdot A_\mathrm{e}}\int_0^t u_\mathrm{s}(\tau)\,\mathrm{d}\tau, \tag{3}$$

where N_s is the number of sense winding turns and A_e the core cross section.

C. Anechoic Chamber

In order to avoid a reflection of the emitted noise at the walls of the measuring room, the acoustic measurements have been conducted in an anechoic chamber. This anechoic chamber has been built for the purpose of this work. The interior of a customary plastic box has been covered with sound-absorbing panels. The internal dimensions are reduced by 3 cm because of these panels. The remaining internal dimensions are then $49.8\,\mathrm{cm}\times39.8\,\mathrm{cm}\times36.2\,\mathrm{cm}$. The DUT is placed centered on a platform of $10\,\mathrm{cm}\times10\,\mathrm{cm}$. Because of the low depth of the sound-absorbing panels (only 3 cm), sound waves of low frequencies are not absorbed well. However, since this work

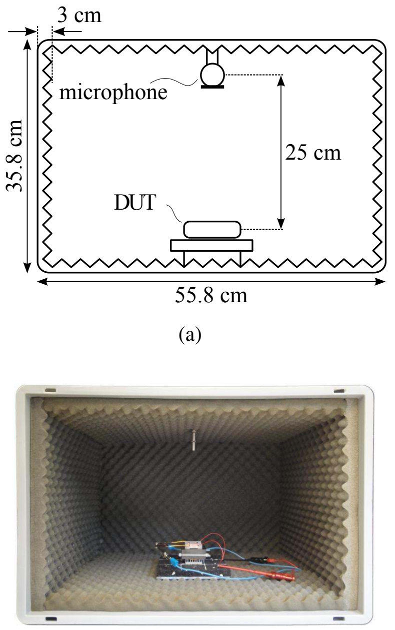

(a)

(b)

Fig. 2. Anechoic chamber: (a) schematic representation; (b) photo.

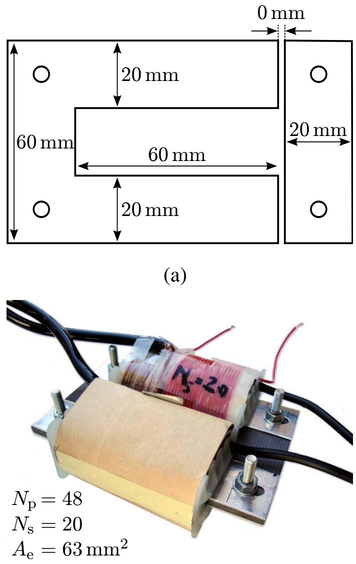

(a)

(b)

Fig. 3. Inductor with a core out of laminated steel. (a) Dimensions of one steel sheet; (b) photo, number of primary winding N_p, number of secondary winding N_s, and cross sectional area A_e of the laminated inductor. A_e is calculated from the limb width of 20 mm and the nine stacked sheets with a thickness of 0.35 mm each.

analyzes the acoustic noise of inductive components operated above 1 kHz, the used sound-absorbing mats are sufficient.

D. Microphone and Frequency Analyzer

The SPL is translated via a microphone into an electric signal. Frequently so-called dynamic microphones are used, which work via electromagnetic induction: the membrane actuates a coil in a magnetic field; the induced voltage is then proportional to the SPL. However, since their operating principle is based on electromagnetic induction, and the DUT has a magnetic stray field, this type of microphones is not suited for this work.

As an alternative, condenser microphones are suitable for the work at hand. They translate the SPL via a plate-capacitor into an electric signal: with a change in the sound pressure, the distance between the plates and, accordingly, the capacitance is changed. The change in capacitance can be measured.

The used microphone for the built test system is the "ONO SOKKI MI-6410 Sound Intensity Measurement Probe". The microphone is placed in the box such that the distance to the DUT is always 25 cm. The measured signal is amplified with the "ONO SOKKI CF-0610 Microphone Amplifier". The frequency spectrum of the signal is then extracted with the frequency analyzer "ONO SOKKI CF-6400 4-Channel Inteligent FFT Analyzer". The measurement equipment has to be calibrated before conducting measurements; this is done with the "ONO SOKKI MI-0600 Sound Pressure Phase Calibrator".

IV. First Measurement Results

In this section, first measurements that confirm the dependency of the acoustic noise to the square of the flux density B^2 are conducted. Furthermore, the origin of the acoustic noise is determined, i.e. it is determined whether the noise is caused by the windings or by the core. For it, two different DUT have been built: one with a laminated steel core and one with a ferrite core.

The laminated core is built with nine UI sheets (grain-oriented steel, M165-35S, lamination thickness $0.35\,\mathrm{mm}$ [14]). The photo and dimensions of the DUT with the laminated core are given in Fig. 3.

The second DUT is built with two ferrite E-cores (EPCOS Ferrit N27, Core-E55/28/21 [15]) and an air gap with length $l_\mathrm{g} = 1\,\mathrm{mm}$ in the middle limb. Photo and dimensions of the ferrite inductor are given in Fig. 4.

A. Noise Characteristic

If the DUT is driven with a symmetric rectangular voltage, the flux density $B(t)$ has a symmetric triangular profile, as illustrated in Fig. 5(a). As discussed in Section II, the source of sound emission is the mechanical vibrations of core and/or windings, which result in an SPL dependency on the square of the flux density, B^2. As can be seen in Fig. 5(b), the spectrum of $B^2(t)$ consists of only even harmonic components B_n^2 with $n = 2, 4, 6, \ldots$, whereas the second harmonic dominates the frequency spectrum. Accordingly, the SPL should consist of only even harmonics too. First measurements have been conducted in order to confirm this behavior. A rectangular voltage shape with a switching frequency of $f_\mathrm{s} = 5\,\mathrm{kHz}$ has been applied across the two DUT. The voltage amplitude has been selected such that a peak-to-peak flux density of $B_\mathrm{pp} = 0.4\,\mathrm{T}$ results. A spectrum similar as in Fig. 5(b) is expected. In other words, mainly the even multiples of the

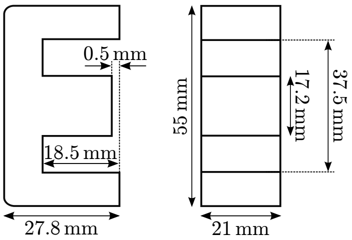

(a)

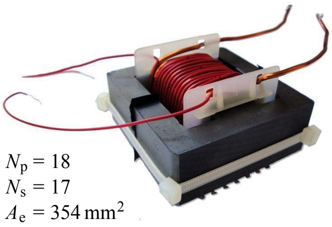

(b)

Fig. 4. Inductor with a ferrite core. (a) Dimensions of the ferrite core; (b) photo, number of primary winding N_p, number of secondary winding N_s, and cross sectional area A_e of the ferrite inductor.

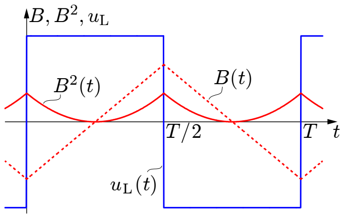

(a)

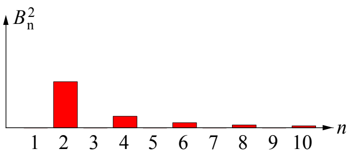

(b)

Fig. 5. Squared magnetic flux density $B^2(t)$ for symmetric excitation. (a) Time domain; (b) harmonic components B_n^2.

switching frequency, i.e. $2 \cdot f_\mathrm{s} = 10\,\mathrm{kHz}$ and $4 \cdot f_\mathrm{s} = 20\,\mathrm{kHz}$ are expected to be measured. Furthermore, it can be expected that the second harmonic $S_{\mathrm{p},2}$ dominates the SPL spectrum.

The measured frequency spectrum of the experiment with the laminated core is given in Fig. 6. As expected, the even harmonics dominate the spectrum. However, the odd harmonics are excited too, though a much lower SPL (at least 27 dB smaller) is measured. The measured frequency spectrum of the experiment with the ferrite core is given in Fig. 7. Here, the odd harmonics are excited even less than in the case of the laminated core.

In both presented frequency spectra the even harmonics are dominant, which seems to confirm that the sound emission is proportional to the square of the magnetic flux density. However, also odd harmonic components have been observed, tough much lower in magnitude. A possible explanation could

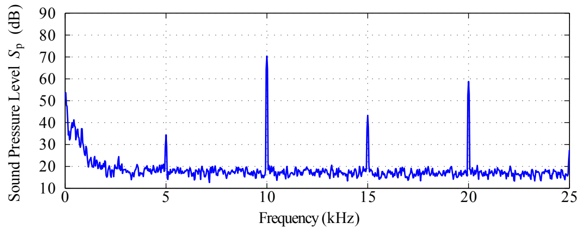

Fig. 6. The measured frequency spectrum of the experiment with a triangular flux density profile with $f_\mathrm{s} = 5\,\mathrm{kHz}$ and $B_\mathrm{pp} = 0.4\,\mathrm{T}$ for the laminated core.

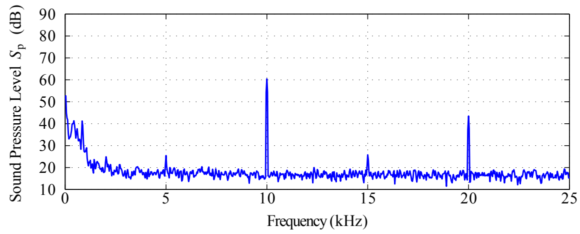

Fig. 7. The measured frequency spectrum of the experiment with a triangular flux density profile with $f_\mathrm{s} = 5\,\mathrm{kHz}$ and $B_\mathrm{pp} = 0.4\,\mathrm{T}$ for the ferrite core.

be that a very small dc bias in the flux density was present in the measurements, which, as will be shown later, leads to odd harmonics in the SPL. Furthermore, the comparably high peak in Fig. 6 at 15 kHz can be explained with the fact that, as will also be shown later, the core at this point exhibits a mechanical resonance.

B. Noise Source

As discussed in Section II, core vibrations are expected to be the dominant noise source, whereas the winding vibrations have a minor influence to the acoustic noise. To confirm this behavior, measurements have been conducted, with and without core, while the current is kept constant. The inductors have been excited such that the current is the same as in the previous measurements. This current shows a triangular profile and peak-to-peak value of $i_\mathrm{pp} = 3.25\,\mathrm{A}$ for the laminated inductor and $i_\mathrm{pp} = 20.1\,\mathrm{A}$ for the ferrite inductor.

In both cases, no measurable noise is emitted without a core, hence, core vibrations are the dominant noise source in

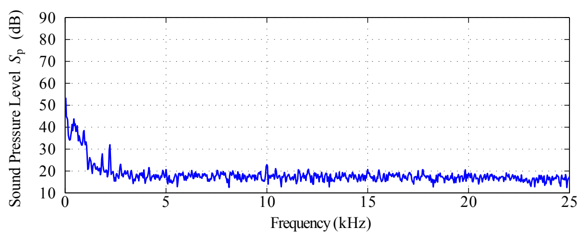

Fig. 8. Frequency spectrum of the experiment with the "ferrite inductor" but without a ferrite core; with peak-to-peak current of $i_\mathrm{pp} = 20.1\,\mathrm{A}$.

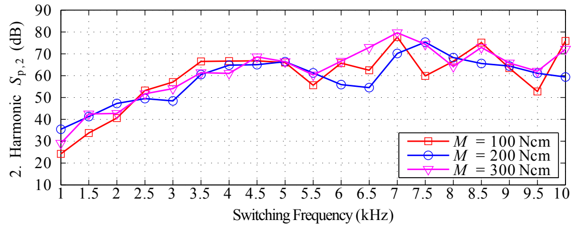

Fig. 9. Second harmonic component of the SPL $S_{\mathrm{p},2}$ of a laminated core as a function of switching frequency f_{s} at different tightening torques M.

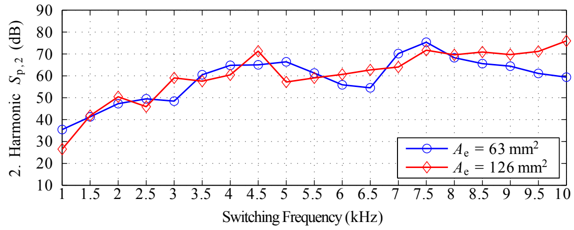

Fig. 10. Second harmonic component of the SPL $S_{\mathrm{p},2}$ of a laminated core as a function of switching frequency f_{s} at different cross sectional areas A_{e}.

the case at hand[1]. In Fig. 8 measurement results for the ferrite inductor but without a ferrite core are given representatively for both DUT. Whether magnetostriction or magnetic forces between core sheets are dominant couldn't be identified with these measurements. The next subsection, therefore, addresses the noise source within the core.

C. Influence of Laminated Core Design on Acoustic Noise

Since core vibrations are the dominant noise source, the configuration of the core will, presumably, have an impact on the sound emission. In the following, it will be investigated whether already simple modifications lead to an improvement of the noise characteristic. This is done on the example of the laminated core. It will be analyzed whether the core volume and, furthermore, the torque with which the screws are tightened influences the sound emission.

In order to determine the influence of the mechanical fixing, three measurements with three different tightening torques have been performed. The four screws as shown in Fig. 3 are tightened with a torque of $M = 100, 200$ and $300\,\mathrm{Ncm}$. In Fig. 9 the measured SPL of the second harmonic $S_{\mathrm{p},2}$ for different switching frequencies and constant $B_{\mathrm{pp}} = 0.4\,\mathrm{T}$, $D = 50\,\%$, and dc-flux-bias $B_{\mathrm{DC}} = 0\,\mathrm{T}$ are given. Although the results are not exactly the same for each torque, no clear dependency between torque and SPL is observed. In fact, it showed that when the core is disassembled and assembled again the core's noise characteristic is (slightly) changed. It can be seen that the SPL differs for different frequencies although the flux density is kept the same. This behavior is discussed later in this paper.

The influence of the core volume on the sound emission is analyzed in a second experiment. For it, additional measurements with twice the laminated core volume have been conducted. The number of lamination sheets is doubled from 9 to 18 accordingly; this leads to a cross sectional area of $A_{\mathrm{e}} = 126\,\mathrm{mm}^2$. The flux density is kept the same, i.e. the flux in the core is doubled too. In Fig. 10 the measured SPL of the second harmonic $S_{\mathrm{p},2}$ for different frequencies and constant $B_{\mathrm{pp}} = 0.4\,\mathrm{T}$, $D = 50\,\%$, and $B_{\mathrm{DC}} = 0\,\mathrm{T}$ are given. Also in this experiment, although the results are not exactly the same for both volumes, no clear dependency between volume and

[1]It could be argued that the core influences the magnetic field between the windings, and, accordingly, the forces between windings change. However, this effect is orders of magnitude smaller than the difference in noise emission with and without core.

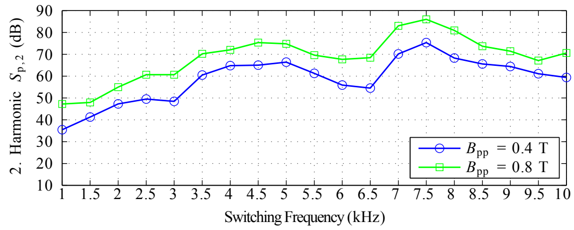

Fig. 11. Second harmonic component of the SPL $S_{\mathrm{p},2}$ of a laminated core as a function of switching frequency f_{s} at different peak-to-peak flux densities B_{pp}.

SPL is observed. This means that, if a specified inductor is built with higher volume (but the flux is kept constant and the flux density is reduced accordingly), a lower SPL is achieved. This is a trivial solution to reduce acoustic noise.

The sound emission was almost independent to changes in the tightening torque. This leads to the assumption that, in the case at hand, the dominant noise source is magnetostriction. Magnetic forces between sheets would result in sheets clashing against each other and, accordingly, to noise. If this would lead to measurable acoustic noise, the tightening torque should have an influence on the sound emission. Since this is not the case, the dominant noise source is presumably the magnetostriction. Whether this conclusion is valid in general, or only for the particular case, has to be investigated as part of a future research.

V. Influence of Flux Profiles on Acoustic Noise

In the previous section, first measurements have confirmed that the SPL shows a dependency on the square of the flux density B^2 and, furthermore, that the dominant noise source is the magnetostriction. In this section, the influence of different flux profiles on the acoustic noise is analyzed. The influence of the frequency f_{s}, a DC premagnetization B_{DC}, and the duty cycle D is analyzed. In all measurements, the flux density has been chosen such that the core is not saturating.

A. Influence of the Switching Frequency to Acoustic Noise

As has been observed in the previous section, the SPL differs for different frequencies, although the flux density is kept the same. Although the core is mechanically exited proportionally to the square of the magnetic flux density $B^2(t)$, the resulting vibrations depend on the frequency.

In Fig. 11 the measured SPL of the second harmonic $S_{\mathrm{p},2}$ as a function of the frequency f_{s} at different peak-to-peak

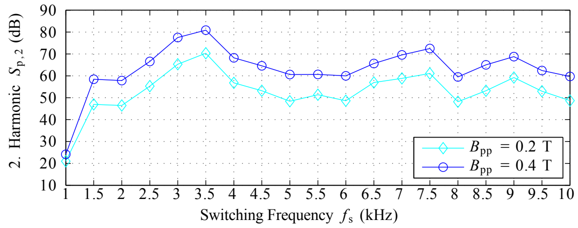

Fig. 12. Second harmonic component of the SPL $S_{p,2}$ of a ferrite core as a function of switching frequency f_s at different peak-to-peak flux densities B_{pp}.

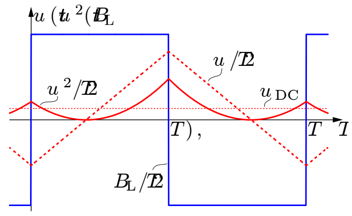

(a)

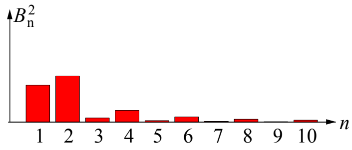

(b)

Fig. 13. Squared magnetic flux density $B^2(t)$ for an excitation with a dc bias of $B_{DC} = 0.2 \cdot B_{pp}$. (a) Time domain; (b) harmonic components B_n^2.

flux densities ($B_{pp} = 0.4\,T$ / $0.8\,T$) and with $D = 50\,\%$ and $B_{DC} = 0\,T$ are given for the laminated core. Two maxima at $f_s \approx 5\,kHz$ and $\approx 7.5\,kHz$ are observed. These maxima are, most likely, due to the mechanical self-resonance of the magnetic core. The resonance frequency of a single lamination sheet has been analyzed in [7], where a single lamination sample of a grain-oriented steel has been fixed on one end and vibrations under sinusoidal excitations with different frequencies have been measured. The experimentally determined resonance frequency showed a good agreement with the analytically calculated resonance frequency. The resonance frequency f_n of a sample that is clamped at one end can be calculated analytically with the modulus of elasticity E ($^N/_{m^2}$), the density ρ ($^{kg}/_{m^3}$) and its length l (m) as

$$f_n = \frac{n}{4 \cdot l}\sqrt{\frac{E}{\rho}}. \quad (4)$$

It is possible to consider the sheet of this work as a sample that is fixed on one end. Hence, its resonance frequency can be calculated with (4). The length in the case at hand is $l = 6\,cm$ and the material parameters are $E = 110\,GPa$ and $\rho = 7650\,^{kg}/_{m^3}$. The material parameters have been extracted from [7]. The first resonance frequency is calculated with $n = 1$ in (4) as $f_1 = 15.8\,kHz$. A switching frequency in the range of $f_s = 7.5\,kHz$ excites the core at $2 \cdot f_s = 15\,kHz$. Accordingly, one can assume that the observed maxima of the second harmonics $S_{p,2}$ at a switching frequency in the range of $f_s = 7.5\,kHz$ is due to the mechanical self-resonance of the magnetic core. Of course, the model to determine the resonance frequency that has been used for this experiment is only a rough estimation. However, for a first approximation it seems to work fairly well.

In Fig. 12 the measured second harmonic $S_{p,2}$ of the SPL for the ferrite core are given as a function of the frequency f_s at different peak-to-peak flux densities ($B_{pp} = 0.2\,T$ / $0.4\,T$) and with $D = 50\,\%$ and $B_{DC} = 0\,T$. The measured SPL show a frequency dependent behavior too. Again, two maxima are found, which are at $f_s \approx 3.5\,kHz$ and $\approx 7.5\,kHz$. Presumably, these maxima are due to the mechanical self-resonance of the magnetic core as well.

B. Influence of a DC Premagnetization on Acoustic Noise

In power electronic systems the magnetic core is often operated under dc bias conditions; this means that a dc magnetic flux, i.e. a dc premagnetization, is present. The influence of such a DC premagnetization on the SPL spectrum is, therefore, investigated in the following.

When considering the dc biased flux profile and its noise producing quantity $B^2(t)$, cf. Fig. 13(a), one recognizes that the profile of $B^2(t)$ is not periodical to half the period of $B(t)$ anymore, but to the period of $B(t)$. In other words, in the spectrum of $B^2(t)$ components at switching frequency and at all odd harmonics are present too. This can be seen in Fig. 13(b). The frequency components of B_n^2 are calculated as

$$B_n^2 = \begin{cases} \dfrac{8 \cdot B_{DC} \cdot B_{pp}}{\pi^2 \cdot n^2} & \text{if } n = 1, 3, 5, \ldots, \\ \dfrac{4 \cdot B_{pp}^2}{\pi^2 \cdot n^2} & \text{if } n = 2, 4, 6, \ldots \end{cases} \quad (5)$$

The even frequency components are not affected by a dc bias, the odd components, however, show a linear correlation to the dc bias B_{DC}.

In order to confirm the above described behavior, measurements at different premagnetization levels have been conducted. The DUT are excited with a switching frequency of $f_s = 5\,kHz$ and a voltage such that a magnetic flux density of $B_{pp} = 0.2\,T$ results. In order to set the dc bias B_{DC}, the according dc current i_{DC} is calculated. For the purpose of simplification, the magnetic flux is considered to depend linearly on the magnetic field strength, and, consequently, linearly to the current. The dc current i_{DC} can then be controlled by the test system. Measurements have been conducted at four different values of B_{DC}, which are $B_{DC} = 0.05, 0.1, 0.15$ and $0.2\,T$. Normalized to B_{pp}, this is $B_{DC} = 0.25, 0.5, 0.75$ and $1.0 \cdot B_{pp}$.

The results for the laminated inductor are shown in Fig. 14, and for the ferrite inductor in Fig. 15. In both plots, the SPL of the first three harmonics $S_{p,1}$, $S_{p,2}$, and $S_{p,3}$ are given. The second harmonic remains (almost) unaffected by a dc bias; this is expected according to (5). The odd harmonics $S_{p,1}$ and $S_{p,3}$ show a linear behavior, as expected according to (5) (a linear

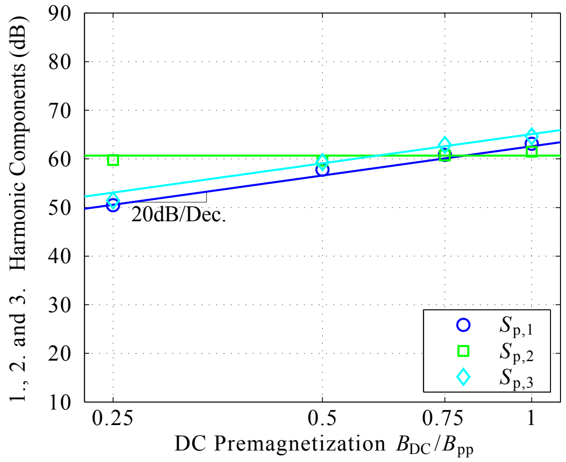

Fig. 14. Harmonic components of the SPL $S_{p,1}$, $S_{p,2}$ and $S_{p,3}$ of a laminated core as a function of the dc premagnetization B_{DC}.

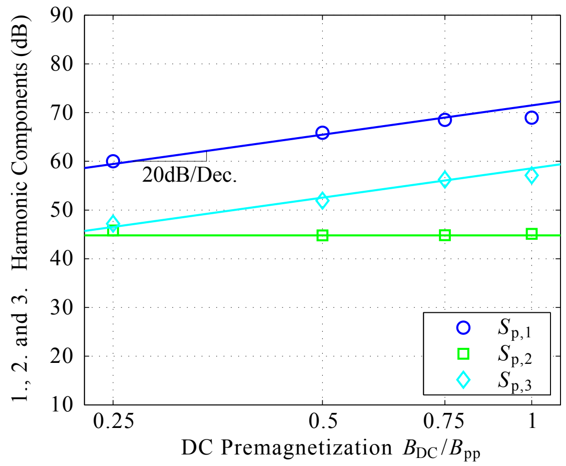

Fig. 15. Harmonic components of the SPL $S_{p,1}$, $S_{p,2}$ and $S_{p,3}$ of a ferrite core as a function of the dc premagnetization B_{DC}.

function in a log-log plot has a slope of 20 dB per decade). In the case of the laminated core, the third harmonic component $S_{p,3}$ has a higher SPL than the first harmonic component $S_{p,1}$. This is because of the frequency dependent behavior, as has been discussed earlier in this paper.

The fact that odd harmonic components are excited in case the core is operated under dc bias conditions may become important in the design phase of inductive components. For instance, the emitted tone with a dc bias is at half the frequency compared to the case without a dc bias; this tone could then be in the audible range.

C. Influence of the Duty Cycle on Acoustic Noise

The influence of the duty cycle D on acoustic noise is analyzed next. Fig. 16(a) shows the waveform of $B^2(t)$ at a duty cycle of $D = 20\,\%$. It can be seen in Fig. 16(b) that for a duty cycle $D \neq 50\,\%$ odd frequency components are present too. Accordingly, the duty cycle D has an influence on the emitted noise. In order to verify this, the DUT have been excited with rectangular voltage waveforms with switching

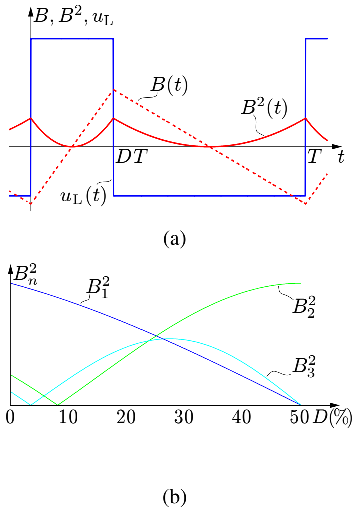

Fig. 16. Squared magnetic flux density $B^2(t)$. (a) Waveform in time domain for an excitation with a duty cycle $D = 20\,\%$; (b) harmonic components B_1^2, B_2^2 und B_3^2 as a function of duty cycle.

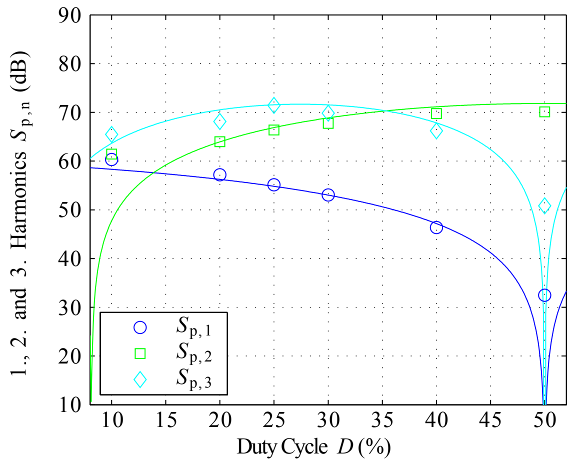

Fig. 17. Measured (dots) and calculated (line) SPL of the first three harmonics $S_{p,1}$, $S_{p,2}$ und $S_{p,3}$ as a function of the duty cycle D for the laminated core.

frequency $f_s = 5\,\text{kHz}$ and duty cycles $D = 10, 20, 25, 30, 40$ and $50\,\%$. The voltage amplitude has been adjusted such that a peak-to-peak flux density $B_{pp} = 0.4\,\text{T}$ results. A series capacitor guarantees that the mean voltage is zero and, accordingly, the current shows no dc component.

In Fig. 17 the measured (dots) and calculated (line) SPL of the first three harmonics as a function of the duty cycle D for the laminated core are given. The measured and calculated SPL results of the ferrite core are given in Fig. 18. For both materials, the calculated values have been calibrated at measurements with a duty cycle of $D = 25\,\%$ and a direct proportionality of $S_{p,n}$ and $B_n^2(t)$ has been assumed.

The measured and calculated values agree reasonably well. A larger difference is only given for duty cycles where the calculations predict very low values of acoustic noise.

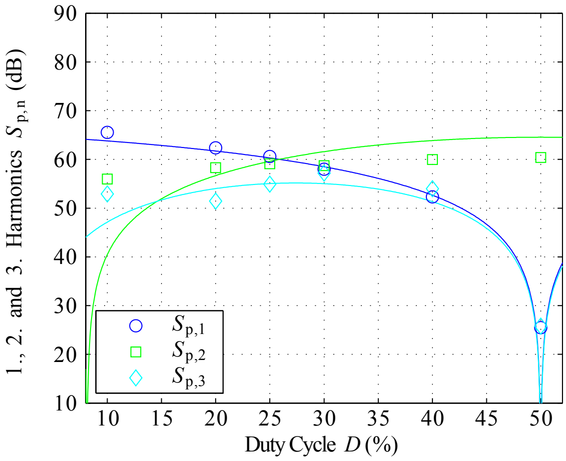

Fig. 18. Measured (dots) and calculated (line) SPL of the first three harmonics $S_{\mathrm{p},1}$, $S_{\mathrm{p},2}$ und $S_{\mathrm{p},3}$ as a function of the duty cycle D for the ferrite core.

VI. Conclusion and Future Work

Power electronic systems that are operated with a switching frequency within the audible frequency range often emit a disturbing acoustic noise, whereas the inductive components are an important source of these noise emissions. This paper dealt with the acoustic emissions of PWM-operated inductive components in the medium frequency range ($\approx 1 \ldots 20\,\mathrm{kHz}$).

It has been shown, how a measurement setup can be built that enables the measurement of the Sound Pressure Level (SPL) spectra of a DUT. With this test setup, SPL spectra of two prototypes have been measured and analyzed. The influence of various modulation parameters, such as the peak-to-peak flux density B_{pp}, the frequency f_{s}, a DC premagnetization B_{DC}, and the duty cycle D, has been investigated. It has been confirmed that the emitted sound is proportional to the square of the magnetic flux density. It has been shown that this noise emissions are primarily caused by magnetostriction.

In a next step, a model should be established that allows to predict the emitted noise already in the design phase of inductive components.

References

[1] B. Weiser, H. Pfützner, and J. Anger, “Relevance of magnetostriction and forces for the generation of audible noise of transformer cores,” *IEEE Transactions on Magnetics*, vol. 36, pp. 3759 –3777, Sep. 2000.

[2] T. D. Gordy, “Audible noise of power transformers,” *Transactions of the American Institute of Electrical Engineers*, vol. 69, pp. 45 –53, Jan. 1950.

[3] A. Moses, P. Anderson, T. Phophongviwat, and S. Tabrizi, “Contribution of magnetostriction to transformer noise,” in *Proc. of the 45th International Universities Power Engineering Conference (UPEC)*, pp. 1 –5, Sep. 2010.

[4] H. Ma, J. He, B. Zhang, R. Zeng, S. Chen, and L. Cao, “Experimental study on dc biasing impact on transformer’s vibration and sound,” in *IEEE International Symposium on Electromagnetic Compatibility*, pp. 1 –4, Aug. 2008.

[5] A. Kelley, “Measurement of spacecraft power transformer acoustic noise,” *IEEE Transactions on Magnetics*, vol. 26, pp. 281 –289, Jan. 1990.

[6] S. Schmitt, “Acoustic noise of sheeted electrical steel inductors in PWM operation’s causes and mitigation,” in *Proc. of the 13th European Conference on Power Electronics and Applications*, pp. 1 –8, Sep. 2009.

[7] T. Phway and A. Moses, “Magnetisation-induced mechanical resonance in electrical steels,” *Journal of Magnetism and Magnetic Materials*, vol. 316, no. 2, pp. 468 – 471, 2007.

[8] W. Lo, C. Chan, Z. Zhu, L. Xu, D. Howe, and K. Chau, “Acoustic noise radiated by PWM-controllel induction machine drives,” *IEEE Transactions on Industrial Electronics*, vol. 47, pp. 880 –889, Aug. 2000.

[9] D. Cameron, J. Lang, and S. Umans, “The origin and reduction of acoustic noise in doubly salient variable-reluctance motors,” *IEEE Transactions on Industry Applications*, vol. 28, pp. 1250 –1255, Nov./Dec. 1992.

[10] C.-Y. Wu and C. Pollock, “Analysis and reduction of vibration and acoustic noise in the switched reluctance drive,” *IEEE Transactions on Industry Applications*, vol. 31, pp. 91 –98, Jan./Feb. 1995.

[11] B. Cullity and C. Graham, *Introduction to magnetic materials*. Wiley-IEEE Press, 2011.

[12] J. Mühlethaler, J. Biela, J. W. Kolar, and A. Ecklebe, “Core losses under the DC bias condition based on Steinmetz parameters,” *IEEE Transactions on Power Electronics*, vol. 27, pp. 953–963, Feb. 2012.

[13] D. Raichel, *The science and applications of acoustics*. Amer. Inst. of Physics, 2000.

[14] “Datasheet to grain oriented steel M165-35S; http://www.wagnergrimm.ch, 14.12.2012.”

[15] “Datasheet to core E55/28/21 out of material EPCOS ferrite N27; http://www.epcos.com, 14.12.2012.”